Preprints of the 21st IFAC World Congress (Virtual)
Berlin, Germany, July 12-17, 2020

Parallel-triggered observer-based output feedback stabilization of linear systems ⋆

Zhiying Wu *,*** **Wei Ren** ** **Junlin Xiong** * **Min Xie** ***

* *Department of Automation, University of Science and Technology of China, Hefei 230026, China (e-mail: junlin.xiong@gmail.com)*
** *Decision and Control Systems, EECS, KTH Royal Institute of Technology, Stockholm, Sweden*
*** *Department of Systems Engineering and Engineering Management, City University of Hong Kong, Kowloon, Hong Kong*

Abstract: Based on the parallel-triggered scheme, the stabilization problem is investigated for linear systems. By utilizing both the absolute and relative errors, a continuous parallel-triggered scheme is proposed. The proposed scheme reduces the number of data transmissions as well as maintains control performance. Under the proposed scheme, Zeno behavior can be excluded. Then, by using Lyapunov theory, sufficient criteria are established for the existence of state feedback controller and the observer-based controller. Next, a co-design approach is provided to obtain both weighting matrix of the triggered scheme and the gain of controller. Finally, the superiority of the proposed scheme is demonstrated by a numerical example.

Keywords: Co-design, event-triggered scheme, observer, stabilization.

1. INTRODUCTION

Digital control methods have been widely applied in practical control systems over the last three decades (Phillips and Nagle, 2007; Isermann, 2013), where control signals are calculated by using sampled data. Many theoretical results of sampled-data control systems have been derived in (Ren and Xiong, 2016; Wang et al., 2018). Sampled-data control method contains event-triggered schemes (ETSs) and time-triggered schemes. Under time-triggered schemes, control signals are updated within a fixed period. However, when event-triggered conditions (ETCs) under ETSs are satisfied, control signals are transmitted. Compared with time-triggered schemes, ETSs can reduce transmission cost.

Event-triggered control problems have received considerable attention (Wu et al., 2020a; Yan et al., 2016; Wu et al., 2020b). In terms of ETCs, the ETSs can be classified into three types: the absolute, the relative, and the mixed ETSs. In absolute ETSs, ETCs are related to absolute errors. Specifically, an absolute ETS was presented in (Zhang and Feng, 2014) by using an exponentially decreasing threshold function. In relative ETSs, ETCs are related to relative errors. To mention a few, an relative ETS was proposed in (Tabuada, 2007), where the state feedback control problems were investigated. To further reduce data transmissions, a mixed ETS is proposed in (Donkers and Heemels, 2012) by using the information of the sum of the relative and absolute errors. Furthermore, a periodic parallel-triggered scheme (PTS) is presented in (Wu et al., 2019) by using both the relative and absolute errors. However, continuous measurements can be used to improve the control performance (Sun et al., 2017; Selivanov and Fridman, 2016). Therefore, it is still open to design a new scheme to further reduce the number of transmitted signals (NTS) as well as maintain the control performance.

In this paper, a novel PTS is proposed. Only when the following two conditions are satisfied, control signals are updated in our PTS. One is the absolute ETC, the other is the relative ETC. The PTS in (Wu et al., 2019) uses the periodic measurements, whereas the proposed PTS uses continuous measurements. Then, the parallel-triggered state feedback and observer-based output feedback stabilization problems are investigated for linear systems. The following challenges are involved: Firstly, different from the results in (Wu et al., 2019), it is not straightforward to ensure that the minimal inter-event interval is positive in continuous PTS. Secondly, under the proposed PTS, the system is either under the absolute ETS or under the relative ETS. However, the methods in (Tabuada, 2007; Zhang and Feng, 2014) are not applicable to this case. Thirdly, it is desirable to co-design both weighting matrix of continuous PTS and the observer-based controller gain. In this paper, the analyses on the minimal inter-event interval are performed. Then, a common Lyapunov function is developed for the system to be investigated. Sufficient criteria are derived for system stability and controller design according to Lyapunov theory. Finally, an example illustrates the superiority of the continuous PTS.

In the paper, the key contributions are as follows: 1) A continuous PTS is proposed for linear systems. The proposed PTS reduces NTS while maintaining the control performance. The advantages are shown via an example. 2) We investigate the case where the system state is unmeasurable. Under the observer-based PTS, we prove

⋆ Junlin Xiong is the corresponding author. This work was supported by National Natural Science Foundation of China (No. 61773357 and 71971181).

that there exists a positive minimal inter-event interval to avoid Zeno behavior. 3) A co-design method is developed to obtain both weighting matrix of continuous PTS and controller gain.

Notation: $\lambda_{\max}(X)$ ($\lambda_{\min}(X)$) represents the maximal (minimal) eigenvalue of X. $\mathbb{N}$ denotes the set of nonnegative integers. I_m denotes the $m \times m$ identity matrix.

2. PROBLEM DESCRIPTION

Consider the system:

$$\begin{cases} \dot{x}(t) = Ax(t) + Bu(t), \\ y(t) = Cx(t), \end{cases} \tag{1}$$

where $x(t) \in \mathbb{R}^n$ is the state, $y(t) \in \mathbb{R}^q$ is the output, and $u(t) \in \mathbb{R}^m$ is the input. Assume that there exist L and K such that $A - LC$ and $A + BK$ are Hurwitz.

The framework of a system under the PTS is demonstrated in Fig. 1. The sensor needs continuous measurements of the system state. The event generator under the PTS decides whether the current system state is transmitted.

To ensure stabilization of the system (1), the controller is given by

$$u(t) = Kx(t_k), \quad t \in [t_k, t_{k+1}), \tag{2}$$

where $K \in \mathbb{R}^{m\times n}$ denotes the gain of controller, and t_k is the latest triggering instant. Assume that $t_0 = 0$.

For $t \in [t_k, t_{k+1})$, define $e(t) \triangleq x(t) - x(t_k)$. By using both relative and absolute errors, a novel continuous parallel-triggered condition (PTC) is presented as follows:

$$\begin{cases} e^T(t)\Phi e(t) \geq \delta x^T(t)\Phi x(t), & \text{(3a)} \\ e^T(t)\Phi e(t) \geq \gamma(t), & \text{(3b)} \end{cases}$$

where $\Phi > 0$ denotes a weighting matrix, $\delta \in (0, 1)$ is a scalar, and $\gamma(t) = c\varepsilon^{-\alpha t}$ with $c > 0$, $\alpha > 0$, and $\varepsilon > 1$. The system state is transmitted when two conditions in (3) are satisfied. Therefore, the proposed PTS is given by:

$$t_{k+1} = \min_{t>t_k}\{t|e^T(t)\Phi e(t) \geq \max\{\delta x^T(t)\Phi x(t), \gamma(t)\}\}. \tag{4}$$

It follows from (4) that if $\gamma(t) > \delta x^T(t)\Phi x(t)$, then the system is under the absolute ETS, otherwise, the system is under the relative ETS. The minimal inter-event intervals under the PTS (4) is not lower than those in (Tabuada, 2007; Lunze and Lehmann, 2010; Zhang and Feng, 2014), see Theorem 3.1.

Remark 2.1. The PTS (4) is a generalization of absolute ETSs in (Lunze and Lehmann, 2010; Zhang and Feng, 2014) and relative ETS in (Tabuada, 2007). Specifically, if $c \to 0^+$, $\delta \in (0, 1)$ and $\Phi = I_n$, the PTS (4) is simplified as the relative ETS in (Tabuada, 2007). If $\delta \to 0^+$, $c > 0$ and $\Phi = I_n$, the PTS (4) is reduced to the absolute ETS in (Lunze and Lehmann, 2010; Zhang and Feng, 2014).

Then, for $t \in [t_k, t_{k+1})$, the system becomes

$$\begin{aligned} \dot{x}(t) &= Ax(t) + Bu(t_k) \\ &= (A + BK)x(t) - BKe(t). \end{aligned} \tag{5}$$

The goal of this paper is to determine the controller (2) to guarantee system stability for the system (5) under the PTS (4).

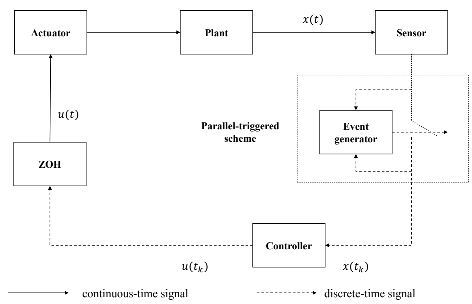

Fig. 1. The framework of a linear system under the PTS

3. PARALLEL-TRIGGERED STATE FEEDBACK CONTROL

In this section, Zeno behavior are ruled out under the PTS (4). Then, sufficient conditions are established for system stability of the system (5). Finally, a co-design method is developed for both weighting matrix and controller gain.

3.1 Analysis on the minimal inter-event interval

Since the PTS (4) depends on continuous supervision, we need to explain that there exists a positive minimal inter-event interval under the PTS (4) to avoid Zeno behavior.

Theorem 3.1. Consider the system (5). The minimal inter-event interval is strictly greater than zero under the PTS (4).

Proof 1. Firstly, similar with the proof of Theorem 5 in (Zhang and Feng, 2014), we prove that $t_{k+1}^{\mathrm{AETS}} - t_k > 0$ for a given state $x(t_k)$, where t_{k+1}^{AETS} is the next triggering instant decided by the absolute ETC (3b).

Next, we show that it is true that $t_{k+1}^{\mathrm{PTS}} \geq t_{k+1}^{\mathrm{AETS}}$ for a given state $x(t_k)$, where t_{k+1}^{PTS} represents the next triggering instant under the PTS (4). Conversely, assume that $t_{k+1}^{\mathrm{PTS}} < t_{k+1}^{\mathrm{AETS}}$. Then based on the absolute ETC (3b), we have

$$e^T(t_{k+1}^{\mathrm{PTS}})\Phi e(t_{k+1}^{\mathrm{PTS}}) < \gamma(t_{k+1}^{\mathrm{PTS}}). \tag{6}$$

Furthermore, noticing (4), we obtain

$$e^T(t_{k+1}^{\mathrm{PTS}})\Phi e(t_{k+1}^{\mathrm{PTS}}) \geq \max\{\delta x^T(t_{k+1}^{\mathrm{PTS}})\Phi x(t_{k+1}^{\mathrm{PTS}}), \gamma(t_{k+1}^{\mathrm{PTS}})\}, \tag{7}$$

which contradicts (6). Therefore, $t_{k+1}^{\mathrm{PTS}} \geq t_{k+1}^{\mathrm{AETS}}$, i.e. $t_{k+1}^{\mathrm{PTS}} - t_k \geq t_{\min} > 0$. This completes the proof.

3.2 Stability analysis

Theorem 3.2. Consider the system (5). For given scalar $\delta \in (0, 1)$, matrices $K \in \mathbb{R}^{m\times n}$ and $\Phi \in \mathbb{R}^{n\times n} > 0$, if there exists a matrix $P \in \mathbb{R}^{n\times n} > 0$ such that

$$\begin{bmatrix} P(A + BK) + (A + BK)^T P + \delta\Phi & PBK \\ \star & -\Phi \end{bmatrix} < 0, \tag{8}$$

then the system (5) under the PTS (4) is globally asymptotically stable.

Proof 2. Let $V(t) = x^T(t)Px(t)$ be the Lyapunov candidate function. For $t \in [t_k, t_{k+1})$, the error $e(t)$ caused by the PTS (4) satisfies

$$e^T(t)\Phi e(t) < \max\{\delta x^T(t)\Phi x(t), \gamma(t)\}. \tag{9}$$

According to the PTS (4), the system (5) is either under the absolute ETS or under the relative ETS. Therefore, this proof is classified as two cases.

Case 1: $\gamma(t) \leq \delta x^T(t)\Phi x(t)$. Then, the system (5) is under the relative ETS. Therefore, we obtain

$$e^T(t)\Phi e(t) < \delta x^T(t)\Phi x(t). \tag{10}$$

Calculating $\dot{V}(t)$, we have

$$\begin{aligned}\dot{V}(t) \leq\ & x^T[(A+BK)^TP + P(A+BK) \\ &+ PBK\Phi^{-1}K^TB^TP]x(t) + e^T(t)\Phi e(t).\end{aligned} \tag{11}$$

From (10) and (11), we obtain

$$\dot{V}(t) \leq x^T Q_1 x(t), \tag{12}$$

where $Q_1 \triangleq P(A+BK)+(A+BK)^TP+PBK\Phi^{-1}K^TB^TP + \delta\Phi$.

Note that the inequality (8) is equivalent to $Q_1 < 0$. In the light of (12), we have

$$\dot{V}(t) \leq -\theta_1 V(t), \quad t \in [t_k, t_{k+1}), \tag{13}$$

where $\theta_1 = \frac{\lambda_{\min}(-Q_1)}{\lambda_{\max}(P)} > 0$.

Case 2: $\gamma(t) > \delta x^T(t)\Phi x(t)$. Using the similar deduction of the first case, we have

$$\begin{aligned}\dot{V}(t) &\leq -\beta_1 V(t) + c\varepsilon^{-\alpha t} \\ &< -\theta_1 V(t) + c\varepsilon^{-\alpha t}, \quad t \in [t_k, t_{k+1}),\end{aligned} \tag{14}$$

where $\beta_1 = \frac{\lambda_{\min}(-Q_1^{'})}{\lambda_{\max}(P)} > \theta_1 > 0$, and $Q_1^{'} \triangleq (A+BK)^TP + P(A+BK) + PBK\Phi^{-1}K^TB^TP < Q_1 < 0$.

Based on (13) and (14) in two cases, we obtain

$$\begin{aligned}\dot{V}(t) &< \max\{-\theta_1 V(t), -\theta_1 V(t) + c\varepsilon^{-\alpha t}\} \\ &= -\theta_1 V(t) + c\varepsilon^{-\alpha t}, \quad t \in [t_k, t_{k+1}),\end{aligned} \tag{15}$$

Then, similar with the derivation of Theorem 1 in (Wu et al., 2019), the global asymptotical stability of the system (5) is guaranteed. This completes the proof.

Remark 3.3. From Theorem 3.2, the stability of the system (5) is dependent on the values δ and Φ, and is unrelated to the values c, α and ε. After choosing the parameters δ and Φ that guarantee the system stability, the values c, ε and α can be appropriately selected to reduce the NTS.

3.3 Controller design

Based on Theorem 3.2, the controller is designed.

Theorem 3.4. Consider the system (5). For given scalar $\delta \in (0, 1)$, if there exist matrices $X \in \mathbb{R}^{n\times n} > 0$, $\widetilde{\Phi} \in \mathbb{R}^{n\times n} > 0$, and $Y \in \mathbb{R}^{m\times n}$ such that

$$\begin{bmatrix} AS + SA^T + BY + Y^TB^T + \delta\widetilde{\Phi} & BY \\ \star & -\widetilde{\Phi}\end{bmatrix} < 0, \tag{16}$$

then the system (5) under the PTS (4) is globally asymptotically stable with $K = YS^{-1}$.

Proof 3. Define $S = P^{-1}$, $Y = KX$ and $S\Phi S = \widetilde{\Phi}$. By pre-multiplying and pos-multiplying (8) with diag$\{S, S\}$ and its transpose, the inequality (16) can be derived from the inequality (8). This completes the proof.

Remark 3.5. The controller gains are required in (Tabuada, 2007; Sun et al., 2017) to be given in advance. However, both controller gain and weighting matrix can be obtained by using Theorem 3.4. The co-design approach in this paper has more applications in practice.

4. PARALLEL-TRIGGERED OBSERVER-BASED OUTPUT FEEDBACK CONTROL

In this section, we investigate the situation where the state is not available. If the system state is unknown, then the state measurement is applied. The state observer is described as

$$\dot{\hat{x}}(t) = A\hat{x}(t) + L(y(t) - C\hat{x}(t)) + Bu(t), \tag{17}$$

where $\hat{x}(t) \in \mathbb{R}^n$ denotes the observer state, and $L \in \mathbb{R}^{n\times q}$ denotes the observer gain.

Then, the controller is given by

$$u(t) = K\hat{x}(\hat{t}_k), \quad t \in [\hat{t}_k, \hat{t}_{k+1}), \tag{18}$$

where $\hat{t}_k$, $k \in \mathbb{N}$, is the latest triggering instant.

For $t \in [\hat{t}_k, \hat{t}_{k+1})$, define $\hat{e}(t) \triangleq \hat{x}(t) - \hat{x}(\hat{t}_k)$. Then, an observer-based PTC is proposed as follows:

$$\begin{cases} \hat{e}^T(t)\Phi\hat{e}(t) \geq \delta\hat{x}^T(t)\Phi\hat{x}(t), & \text{(19a)} \\ \hat{e}^T(t)\Phi\hat{e}(t) \geq \gamma(t), & \text{(19b)}\end{cases}$$

where Φ, δ and $\gamma(t)$ are defined in (3).

Thus, the observer-based PTS is determined by

$$\hat{t}_{k+1} = \min_{t>\hat{t}_k}\{t|\hat{e}^T(t)\Phi\hat{e}(t) \geq \max\{\delta\hat{x}^T(t)\Phi\hat{x}(t), \gamma(t)\}\}. \tag{20}$$

Define $\tilde{x}(t) \triangleq x(t) - \hat{x}(t)$, and $\eta(t) = [x^T(t), \tilde{x}^T(t)]^T$. Similar with the system modeling in (Zhang and Feng, 2014), the investigated system becomes

$$\dot{\eta}(t) = \bar{A}\eta(t) + \bar{B}\hat{e}(t), \quad t \in [\hat{t}_k, \hat{t}_{k+1}), \tag{21}$$

where

$$\bar{A} = \begin{bmatrix} A+BK & -BK \\ 0 & A-LC\end{bmatrix}, \quad \bar{B} = \begin{bmatrix} -BK \\ 0\end{bmatrix}.$$

4.1 Analysis on the minimal inter-event interval

In this subsection, we derive that the minimal inter-event interval is positive under the PTS (20). Thus, Zeno behavior can be avoided.

Theorem 4.1. Consider the system (21). The minimal inter-event interval is not lower than $t_{\min} > 0$ under the PTS (20).

Proof 4. Firstly, we prove that $\hat{t}_{k+1}^{\mathrm{AETS}} - \hat{t}_k > 0$ for given states $x(\hat{t}_k)$ and $\hat{x}(\hat{t}_k)$, where $\hat{t}_{k+1}^{\mathrm{AETS}}$ denotes the next triggering instant under the absolute ETC (19b).

Recalling the upper bound of $\hat{e}(t)$ in (Zhang and Feng, 2014), we have

$$\|\hat{e}(t)\| \leq \phi_2(\hat{t}_k)\int_{\hat{t}_k}^{t} \mathrm{e}^{\|A\|(t-s)}ds, \quad t \in [\hat{t}_k, \hat{t}_{k+1}), \tag{22}$$

where $\phi_2(\hat{t}_k) = \|A+BK\|\|\hat{x}(\hat{t}_k)\| + c\mathrm{e}^{\frac{\lambda_{\max}(A-LC)}{2}\hat{t}_k}\|LC\| \|\widetilde{x}(0)\|$. From (22), we have

$$\sqrt{\hat{e}^T(t)\Phi\hat{e}(t)} \leq \sqrt{\lambda_{\max}(\Phi)}\phi_2(\hat{t}_k)\int_{\hat{t}_k}^{t} \mathrm{e}^{\|A\|(t-s)}ds. \tag{23}$$

Similar with the proof in Theorem 3.1, we can draw that $\hat{t}_{k+1}^{\mathrm{PTS}} \geq \hat{t}_{k+1}^{\mathrm{AETS}}$, where $\hat{t}_{k+1}^{\mathrm{PTS}}$ is the next triggering instant determined by the PTS (20). Therefore, $\hat{t}_{k+1}^{\mathrm{PTS}} - \hat{t}_k \geq t_{\min} > 0$. This completes the proof.

4.2 Stability analysis

Next, sufficient criteria are established for the existence of the observer (17) and the observer-based controller (18) under the PTS (20).

Theorem 4.2. Consider the system (21) under the PTS (20). For given scalar $\delta \in (0,1)$, matrices $K \in \mathbb{R}^{m\times n}$ and $\Phi \in \mathbb{R}^{n\times n} > 0$, if there exist matrices $P_1 \in \mathbb{R}^{n\times n} > 0$ and $P_2 \in \mathbb{R}^{n\times n} > 0$ such that

$$\begin{bmatrix} \Delta_{11} & -P_1BK & I_n & P_1BK \\ \star & \Delta_{22} & -I_n & 0 \\ \star & \star & -\delta^{-1}\Phi^{-1} & 0 \\ \star & \star & \star & -\Phi \end{bmatrix} < 0, \tag{24}$$

where $\Delta_{11} = (A+BK)^TP_1 + P_1(A+BK)$, and $\Delta_{22} = (A-LC)^TP_2 + P_2(A-LC)$, then the global asymptotical stability is guaranteed for the system (21).

Proof 5. Let $V(t) = \eta^T(t)\bar{P}\eta(t)$ be the Lyapunov candidate function, where $\bar{P} = \begin{bmatrix} P_1 & 0 \\ 0 & P_2 \end{bmatrix} > 0$.

For $t \in [\hat{t}_k, \hat{t}_{k+1})$, the error $\hat{e}(t)$ caused by the PTS (20) satisfies

$$\hat{e}^T(t)\Phi\hat{e}(t) < \max\{\delta\hat{x}^T(t)\Phi\hat{x}(t), \gamma(t)\}. \tag{25}$$

According to the PTS (20), the system (21) is either under the absolute ETS or under the relative ETS. Therefore, the proof is classified as two cases.

Case 1: $\gamma(t) \leq \delta\hat{x}^T(t)\Phi\hat{x}(t)$. Then, the system (21) is under the relative ETS. Thus, we obtain

$$\hat{e}^T(t)\Phi\hat{e}(t) < \delta\hat{x}^T(t)\Phi\hat{x}(t) = \eta^T(t)E_2^T\delta E_2\eta(t), \tag{26}$$

where $E_2 = [I_n \ -I_n]$.

The time derivative of $V(t)$ is

$$\dot{V}(t) \leq \eta^T[\bar{A}^T\bar{P} + \bar{P}\bar{A} + \bar{P}\bar{B}\Phi^{-1}\bar{B}^T\bar{P}]\eta(t) + \hat{e}^T(t)\Phi\hat{e}(t). \tag{27}$$

From (26) and (27), we obtain

$$\dot{V}(t) \leq \eta^TQ_2\eta(t), \tag{28}$$

where $Q_2 \triangleq \bar{A}^T\bar{P} + \bar{P}\bar{A} + \bar{P}\bar{B}\Phi^{-1}\bar{B}^T\bar{P} + \delta E_2^T\Phi E_2$.

Note that the inequliaty (24) is rewritten as $Q_2 < 0$. Therefore, we have

$$\dot{V}(t) \leq -\theta_2V(t), \quad t \in [\hat{t}_k, \hat{t}_{k+1}), \tag{29}$$

where $\theta_2 = \frac{\lambda_{\min}(-Q_2)}{\lambda_{\max}(\bar{P})} > 0$.

Case 2: $\gamma(t) > \delta\hat{x}(t)\Phi\hat{x}(t)$. Following the similar derivation of the first case, we have

$$\begin{aligned}\dot{V}(t) &\leq -\beta_2V(t) + c\varepsilon^{-\alpha t} \\ &< -\theta_2V(t) + c\varepsilon^{-\alpha t}, \quad t \in [\hat{t}_k, \hat{t}_{k+1}),\end{aligned} \tag{30}$$

where $\beta_2 = \frac{\lambda_{\min}(-Q_2')}{\lambda_{\max}(\bar{P})} > \theta_2 > 0$, and $Q_2' \triangleq \bar{A}^T\bar{P} + \bar{P}\bar{A} + \bar{P}\bar{B}\Phi^{-1}\bar{B}^T\bar{P} < Q_2 < 0$.

Similar with the proof in Theorem 3.2, the global asymptotical stability is guaranteed for the system (21). This completes the proof.

Remark 4.3. Under the PTS, the observer-based feedback control problem is studied in this paper. The authors of (Sun et al., 2017) consider the parallel-triggered state feedback control problem only. Therefore, our results are more practical.

4.3 Observer and controller design

Based on Theorem 4.2, our goal is to determine an observer-based controller (18) for the system (21) under the PTS (20).

Theorem 4.4. Consider the system (21) under the PTS (20). For given scalars $\delta \in (0,1)$ and $\epsilon > 0$, if there exist matrices $S_1 \in \mathbb{R}^{n\times n} > 0$, $P_2 \in \mathbb{R}^{n\times n} > 0$ and $\Phi \in \mathbb{R}^{n\times n} > 0$, $Y_1 \in \mathbb{R}^{m\times n}$ and $U \in \mathbb{R}^{n\times q}$ such that

$$\begin{bmatrix} \Pi_{11} & 0 & S_1 & 0 & BY_1 & 0 \\ \star & \Pi_{22} & -I_n & 0 & 0 & -I_n \\ \star & \star & \Phi - 2\delta^{-\frac{1}{2}}I_n & 0 & 0 & 0 \\ \star & \star & \star & -\Phi & 0 & I_n \\ \star & \star & \star & \star & -\epsilon^{-1}S_1 & 0 \\ \star & \star & \star & \star & \star & -\epsilon S_1 \end{bmatrix} < 0. \tag{31}$$

where $\Pi_{11} = AS_1 + S_1A^T + BY_1 + Y_1^TB^T$, and $\Pi_{22} = P_2A + A^TP_2 - UC - C^TU^T$, then the global asymptotical stability is guaranteed for the system (21) with $L = P_2^{-1}U$ and $K = Y_1S_1^{-1}$.

Proof 6. Recalling Theorem 4.2, pre-multiplying and post-multiplying (24) with $\mathrm{diag}\{P_1^{-1}, I_n, I_n, I_n\}$ and its transpose, we obtain

$$\begin{bmatrix} \Pi_{11} & 0 & S_1 & 0 \\ \star & \Pi_{22} & -I_n & 0 \\ \star & \star & -\delta^{-1}\Phi^{-1} & 0 \\ \star & \star & \star & -\Phi \end{bmatrix} + \begin{bmatrix} BK \\ 0 \\ 0 \\ 0 \end{bmatrix} E_4 + E_4^T \begin{bmatrix} BK \\ 0 \\ 0 \\ 0 \end{bmatrix}^T < 0, \tag{32}$$

where $S_1 = P_1^{-1}$, $Y_1 = KS_1$, $U = P_2L$, and $E_4 = [0 \ -I_n \ 0 \ I_n]$.

By applying Young inequality, one just ensures

$$\begin{bmatrix} \Pi_{11} & 0 & S_1 & 0 & BY_1 & 0 \\ \star & \Pi_{22} & -I_n & 0 & 0 & -I_n \\ \star & \star & -\delta^{-1}\Phi^{-1} & 0 & 0 & 0 \\ \star & \star & \star & -\Phi & 0 & I_n \\ \star & \star & \star & \star & -\epsilon^{-1}S_1 & 0 \\ \star & \star & \star & \star & \star & -\epsilon S_1 \end{bmatrix} < 0, \tag{33}$$

where ϵ is a positive constant.

Because $(I_n - \delta^{-\frac{1}{2}}\Phi^{-1})^T\Phi(I_n - \delta^{-\frac{1}{2}}\Phi^{-1}) \geq 0$, we have

$$-\delta^{-1}\Phi^{-1} \leq \Phi - 2\delta^{-\frac{1}{2}}I_n. \tag{34}$$

Thus, the condition (31) ensures the condition (24) in Theorem 4.2 is satisfied. From Theorem 4.2, the global asymptotical stability is guaranteed for the system (21). This completes the proof.

Remark 4.5. In (Zhang and Feng, 2014), the controller gains and observer gains are required to be given in advance. In this paper, a co-design approach is provided to obtain weighting matrix of the PTS (20) and observer-based controller gain.

5. ILLUSTRATIVE EXAMPLES

In this section, a pendulum system is presented to demonstrate that the proposed PTS can further reduce NTS compared with the schemes in (Tabuada, 2007; Sun et al., 2017; Zhang and Feng, 2014). Consider a cart with an inverted pendulum investigated in (Tabuada, 2007; Sun et al., 2017; Zhang and Feng, 2014). The state-space equation of the system is described as

$$A = \begin{bmatrix} 0 & 1 & 0 & 0 \\ 0 & \dfrac{-(ml^2+I)b}{Mml^2+I(M+m)} & \dfrac{m^2l^2g}{Mml^2+I(M+m)} & 0 \\ 0 & 0 & 0 & 1 \\ 0 & \dfrac{-mlb}{Mml^2+I(M+m)} & \dfrac{ml(M+m)g}{Mml^2+I(M+m)} & 0 \end{bmatrix},$$

$$B = \begin{bmatrix} 0 \\ \dfrac{ml^2+I}{Mml^2+I(M+m)} \\ 0 \\ \dfrac{ml}{Mml^2+I(M+m)} \end{bmatrix},$$

where I denotes the inertia of the pendulum, M is the cart mass, m represents the mass of the pendulum, b denotes the friction constant of the cart, l is the length of the pendulum, and g is the gravitational acceleration. The state $x = [x_1\ x_2\ x_3\ x_4]^T$, where x_i $(i = 1, 2, 3, 4)$ denote the position and the velocity of cart, the angle and angular velocity of pendulum, respectively. The two cases are investigated as follows. Case 1 and Case 2 are used to show the effectiveness of the state feedback PTS (4) and the observer-based PTS (20), respectively.

Case 1: We set $C = I_4$, $I = 0.006\text{kg}\cdot\text{m}^2$, $m = 0.2\text{kg}$, $l = 0.3\text{m}$, $b = 0.1\text{N/m/s}$, $M = 0.5\text{kg}$, and $g = 9.8\text{m/s}^2$. Moreover, $x(0) = [0.98\ 0\ 0.2\ 0]^T$, and $K = [4.2719\ 5.2115\ -34.0635\ -6.5903]$. The parameters are the same as those in (Sun et al., 2017).

The comparison between the ETSs in (Tabuada, 2007; Zhang and Feng, 2014), the PTS in (Sun et al., 2017) and our PTS (4) is given. The PTS in (Sun et al., 2017) is implemented:

$$\begin{cases} e^T(t)e(t) \geq \delta x^T(t)x(t), & \text{(35a)} \\ x^T(t)x(t) \geq e^{-\lambda(t-t_0)}x^T(t_0)x(t_0), & \text{(35b)} \end{cases}$$

where $0 < \delta < 1$ and $\lambda > 0$ are constants. We consider $\delta = 0.0064$, $\lambda = 1.76$, $\varepsilon = e$, $c = 0.01$, and $\alpha = 2.29$. The results of simulation are shown in Fig. 2. Fig. 2 illustrates that the control performance under our PTS (4) is similar to that under the ETSs in (Tabuada, 2007; Zhang and Feng, 2014), whereas the control performance under the PTS in (Sun et al., 2017) is severely damaged. The corresponding settling time (ST) under four schemes are listed in Table 1, where ST is the time for the system states has accessed and remained within 0.05% error band of the desired states. From Table 1, the ST under the PTS in (Sun et al., 2017) is larger than those in (Tabuada, 2007; Zhang and Feng, 2014) and PTS (4). In Table 1, NTSs under the relative ETS in (Tabuada, 2007), the absolute ETS (Zhang and Feng, 2014), the PTS in (Sun et al., 2017) and our PTS (4) are 227, 160, 144 and 144, respectively. The results show that not only the control performance under the PTS (4) is similar to those in (Tabuada, 2007; Zhang and Feng, 2014), but also the NTS is reduce.

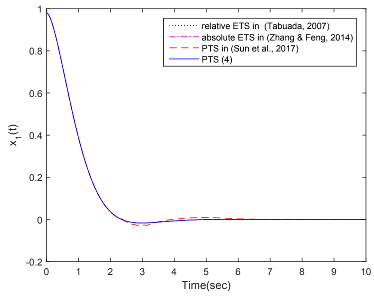

(a) System state $x_1(t)$ under four schemes

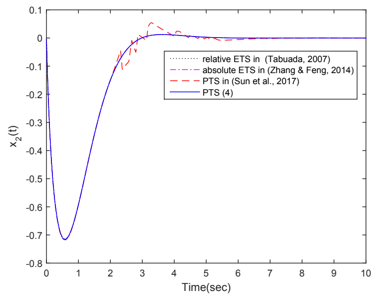

(b) System state $x_2(t)$ under four schemes

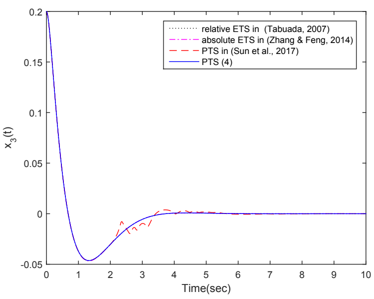

(c) System state $x_3(t)$ under four schemes

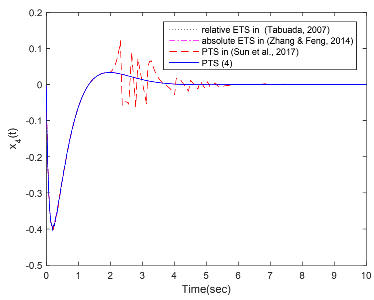

(d) System state $x_4(t)$ under four schemes

Fig. 2. System states under four schemes.

Table 1. NTS and ST under four schemes.

Relative ETS in (Tabuada, 2007)	NTS	227
	ST	2.4708
Absolute ETS in (Zhang and Feng, 2014)	NTS	160
	ST	2.4668
PTS in (Sun et al., 2017)	NTS	144
	ST	3.4215
PTS (4)	NTS	144
	ST	2.4716

Case 2: We set $C = \begin{bmatrix} 1 & 0 & 0 & 0 \\ 0 & 0 & 1 & 0 \end{bmatrix}$, $I = 0.006\text{kg}\cdot\text{m}^2$, $m = 0.5\text{kg}$, $l = 0.3\text{m}$, $b = 0.1\text{N/m/s}$, $M = 0.5\text{kg}$, and $g = 9.8\text{m/s}^2$. Moreover, $x(0) = [0.98\ 0\ 0.2\ 0]^T$ and $\hat{x}(0) = [0.1\ 0\ 0\ 0]^T$. The controller gain is $K = [4.2719\ 5.2115\ -34.0635\ -6.5903]$, and observer gains is given as follows:

$$L = \begin{bmatrix} 11.0993 & -0.0991 \\ 29.7908 & 2.1306 \\ -0.5518 & 11.3189 \\ -5.5941 & 63.2481 \end{bmatrix}.$$

The parameters are the same as those in (Zhang and Feng, 2014).

The comparison results between the ETSs in (Tabuada, 2007; Zhang and Feng, 2014) and the observer-based PTS (20) are presented. For the PTS (20), set $\delta = 0.003$, $\Phi = I_4$, $\varepsilon = e$, $c = 1.0$, and $\alpha = 3.4$. The feasibility of the LMI (24) of Theorem 4.2 is verified. The relative ETS in (Tabuada, 2007) and the absolute ETS in (Zhang and Feng, 2014) are also performed. The NTSs under the relative ETS in (Tabuada, 2007), the absolute ETS (Zhang and Feng, 2014) and our PTS (20) are 431, 482 and 246, respectively. Therefore, our PTS (20) reduces NTS while preserving the control performance.

Next, the co-design approach is used. By using Theorem 4.4 with $\delta = 0.003$ and $\epsilon = 0.01$, we have

$$K = [22.9103\ 32.6736\ -142.5649\ -30.5677],$$

$$L = \begin{bmatrix} 0.7218 & -3.9896 \\ 0.3871 & 6.8740 \\ 3.5637 & 0.9286 \\ 1.1157 & 53.8362 \end{bmatrix},$$

$$\Phi = \begin{bmatrix} 9.7228 & 3.0451 & -4.5188 & -1.0206 \\ \star & 8.2820 & -5.8408 & -3.2707 \\ \star & \star & 30.7953 & 3.9779 \\ \star & \star & \star & 4.8682 \end{bmatrix}.$$

Both weighting matrix of continuous PTS (20) and controller gain are co-designed by Theorem 4.4. However, the controllers are needed to be given a priori in (Tabuada, 2007; Zhang and Feng, 2014). Therefore, the co-design method is more convenient than the methods in (Tabuada, 2007; Zhang and Feng, 2014).

6. CONCLUSIONS

The parallel-triggered stabilization problem was investigated in this paper for linear systems. A continuous parallel-triggered scheme was proposed. Then, sufficient conditions were derived for the system stability and the co-design method. Finally, the simulation results showed that our scheme could further reduce signal transmissions while maintaining the control performance. Future research will be extended to the systems under an adaptive parallel-triggered scheme.

REFERENCES

Donkers, M. and Heemels, W. (2012). Output-based event-triggered control with guaranteed $\mathcal{L}_\infty$-gain and improved and decentralized event-triggering. *IEEE Transactions on Automatic Control*, 57(6), 1362–1376.

Isermann, R. (2013). *Digital Control Systems*. Springer Science & Business Media.

Lunze, J. and Lehmann, D. (2010). A state-feedback approach to event-based control. *Automatica*, 46(1), 211–215.

Phillips, C.L. and Nagle, H.T. (2007). *Digital Control System Analysis and Design*. Prentice Hall Press.

Ren, W. and Xiong, J. (2016). Stability and stabilization of switched stochastic systems under asynchronous switching. *Systems & Control Letters*, 97, 184–192.

Selivanov, A. and Fridman, E. (2016). Event-triggered H_∞ control: A switching approach. *IEEE Transactions on Automatic Control*, 61(10), 3221–3226.

Sun, X.M., Wang, X.F., Hong, Y., and Xia, W. (2017). Stabilization control design with parallel-triggering mechanism. *IEEE Transactions on Industrial Electronics*, 64(4), 3260–3267.

Tabuada, P. (2007). Event-triggered real-time scheduling of stabilizing control tasks. *IEEE Transactions on Automatic Control*, 52(9), 1680–1685.

Wang, Y., Xiong, J., and Ho, D.W. (2018). Decentralized control scheme for large-scale systems defined over a graph in presence of communication delays and random missing measurements. *Automatica*, 98, 190–200.

Wu, Z., Mo, H., Xiong, J., and Xie, M. (2020a). Adaptive event-triggered observer-based output feedback $\mathcal{L}_\infty$ load frequency control for networked power systems. *IEEE Transactions on Industrial Informatics*, 16(6), 3952–3962.

Wu, Z., Wang, Y., Xiong, J., and Xie, M. (2019). Static output feedback stabilization of networked control systems with a parallel-triggered scheme. *ISA Transactions*, 85, 60–70.

Wu, Z., Xiong, J., and Xie, M. (2020b). A switching method to event-triggered output feedback control for unmanned aerial vehicles over cognitive radio networks. *IEEE Transactions on Systems Man and Cybernetics: Systems*. doi:10.1109/TSMC.2020.2971726.

Yan, S., Shen, M., and Zhang, G. (2016). Extended event-driven observer-based output control of networked control systems. *Nonlinear Dynamics*, 86(3), 1639–1648.

Zhang, J. and Feng, G. (2014). Event-driven observer-based output feedback control for linear systems. *Automatica*, 50(7), 1852–1859.